Chapter 2

SOURCE TERM EVALUATIONS

Stephen W. White, Paul P. Whalen, Alexandra R. Heath

Description of the Calculations

This chapter presents an evaluation of the energy and angular distributions of the prompt radiation that was produced by the atomic bombs in Hiroshima and Nagasaki. These "source terms" are calculated quantities produced by computer codes that simulate the explosion of the bomb and track the radiation intensities from production in the interior of the bomb to leakage (escape) at its boundary.

These data contribute, indirectly, to radiation doses to people at ground level. Additional calculations are required to evolve these initial distributions from the epicenter through the air and ground. During this process the radiation can be absorbed and, possibly, re-emitted with a different direction, energy or particle composition. These subsequent calculations are described in Chapter 3. In addition, these calculations were used to provide a simple description of the isotopic composition of the fission debris, from which delayed radiation can be inferred (White 2002).

The atomic bomb that exploded at Hiroshima is often referred to as Little Boy. It had a cylindrical geometry in which two subcritical components were assembled into a supercritical geometry by propelling one toward the other. The fissile components were made of highly enriched uranium. The atomic bomb that exploded at Nagasaki is referred to as Fat Man. It had a spherical geometry in which a subcritical ball of plutonium was compressed to supercriticality by a converging shock wave driven by high explosives.

These source terms have been calculated several times in the past. In particular, Preeg calculated the neutron and gamma-ray output of a 1-dimensional (spherical) mock-up of the Hiroshima device in 1975. These calculational results were declassified and issued as an unclassified letter to C. P. Knowles of R & D Associates (Preeg 1976). In his transmittal letter, Preeg also included calculations of the prompt neutron and gamma-ray doses as a function of range in an air only (no ground plane) configuration. These calculations provided key pieces of information in the events leading up to a reevaluation of atomic-bomb dosimetry for Hiroshima and Nagasaki (Bond and Thiessen 1982).

In 1982 Kammerdiener and Streetman made a more accurate 2-dimensional cylindrical model

of the Hiroshima device at Los Alamos (Whalen 1983, 1987). The results of this 2-dimensional output calculation contained 38 neutron group and 27 gamma ray groups, each divided into 20 directional bins. The current calculations contain 200 neutron groups, 43 gamma ray groups, each of which is divided into 40 directional bins. In general, the current suite of calculations described here incorporates more geometry, more extensive data, higher computational resolution (spatial and temporal), and produces output tabulations with significantly more detail than was possible with the earlier calculations by Kammerdiener and Streetman. In 1982 when the DS86 source calculations were made, computer size and speed made it impossible to include the entire weapon geometry in the calculation. The results were obtained in 1982 by reducing the geometry of the calculation to its essentials and making appropriate adjustments. In the current calculations, a significant effort was undertaken to grid up the entire geometry of the detonation, knowing that computer hardware limitations were almost insignificant compared to including the best physics models and data bases. The transport calculations were run to a final time of one second, which ensures a well-characterized energy spectrum in the newer 2001 calculations for DS02.

Comparisons of some integral quantities between these newer 2001 data and the previous data published in DS86 (Whalen 1987) are presented in Table 1. The entries in this table, which identify a total number, are calculated by integrating *N(E)* over the entire energy range, where *N(E)* is the spectrum in *moles* kt^{-1} MeV^{-1}. (The unit abbreviation, *kt*, refers to the "yield" of the device expressed as the energy released equivalent to the detonation of 1,000 tons of TNT.) The quantities that refer to an average energy are calculated by using the spectrum as a weighting function:

$$< E > = \frac{\int E \cdot N(E) dE}{\int N(E) dE}$$

The calculations were performed by Los Alamos National Laboratory (LANL) computer codes used in the design and characterization of nuclear weapons. The codes have undergone extensive comparison with diagnostic data acquired in atmospheric and underground nuclear tests. In addition to improvements over time in the physics capabilities in these codes, there has been fairly significant improvement in their computational speed. As an example, each of the calculations whose output was published in DS86 took approximately 50 hours of Cray CPU

Table 1. Comparison of integral quantities: DS02 calculations to DS86

Quantity	Units	DS02	DS86	DS02/DS86
Hiroshima				
Total neutrons	moles/kt	0.1768	0.1773	0.9972
Average neutron energy	MeV	0.3106	0.3059	1.0153
Total gamma rays	moles/kt	0.006665	0.005083	1.3113
Average gamma ray energy	MeV	1.3979	1.4137	0.9888
Yield range	kt	15-18		
Nagasaki				
Total neutrons	moles/kt	0.2640	0.2734	0.9657
Average neutron energy	MeV	0.0126	0.0201	0.6269
Total gamma rays	moles/kt	0.09022	0.06296	1.4330
Average gamma ray energy	MeV	1.2667	1.3495	0.9387
Yield range	kt	18-22		

time. Contemporary supercomputers comprise thousands of processing nodes, and parallel-processing adaptations of the LANL codes provided roughly 10^4-10^5 times the processing performance relative to the Cray calculations. Stated in 1982 units, each of the calculations whose output is published in this report would have required 125 Cray-days to complete.

The 2001 calculations all used cross sections processed from the ENDF/B-VI.2 database (McVane 1995, Hendricks 1994). No adjustments were made to these data.

The prompt neutron outputs of these calculations were accumulated into 200 energy bins (Appendix A), and the prompt gamma outputs were accumulated into 43 energy bins (Appendix B). The Hiroshima device, because of its asymmetrical geometry, had these quantities further broken down into 40 angular bins (Appendix C). The selection of both the energy and angular bins was taken from a data set (White et al. 2000) provided by the Oak Ridge National Laboratory (ORNL). One additional neutron group (0 to 1×10^{-11} MeV) and one additional gamma-ray goup (0 to 1×10^{-3} MeV) were added to the ORNL data set for use in the leakage calculations for the Hiroshima and Nagasaki bombs. The neutron and gamma-ray leakages in these very low-energy groups were zero, and only the leakage data in the original 199 neutron groups and 42 gamma-ray groups of ORNL data set were used in the radiation transport calculations (Chapter 3 and Chapter 12, Part A).

The inferred yields of the devices in these calculations are consistent with the range of yield estimates from a variety of other studies (Chapter 1). Specifically, the yield of the Hiroshima device is assessed to be between 14 and 18 kt; the yield of Nagasaki device is assessed to be between 18 and 22 kt.

The uncertainty for the Hiroshima yield is, in part, attributable to not knowing exactly when neutron multiplication began. In this device it was possible to have the configuration reach a supercritical geometry while the assembly was still in progress. Moreover, once the parts reached their final configurations, it was still necessary for a free neutron to be present from which multiplication by fission could proceed in the supercritical geometry. The designers of the device were well aware of the time interval in which the configuration was supercritical and in need of the initial neutron to begin multiplication. In fact, they made estimates of the full device yield as a function of the time at which neutron multiplication began. In an attempt to produce maximum yield, a component referred to as an “initiator” was designed and tested to introduce an initial number of neutrons into the supercritical configuration near the “optimal” time. In an effort to insure that neutron multiplication would begin as nearly as possible to the optimal time in the supercritical configuration, four polonium-beryllium initiators were used instead of just one. While the neutron production rate remains classified, the source strength of the initiators was remeasured on August 5, 1945 and found to be well within design specification.

Despite these efforts at optimization, there is uncertainty in the timing, because stray neutrons are not impossible, the initiators were mechanically activated, and because no diagnostic indicator of the time of the start of multiplication was provided. Uncertainty in the timing translates into an uncertainty in the yield. However, calculations to assess the effect of different times for the start of multiplication gave yields ranging from a low of 15 kt to a high of 18 kt (Table 1). The *number* of neutrons produced by fission will scale linearly with yield, but the *spectrum* will remain invariant within the excursions provided by the yield uncertainty range. For this reason the spectrum is given “per kiloton yield,” and any subsequent analysis is free to scale the yield within the cited uncertainties.

Hiroshima Neutron Source

Figure 1 shows the angle-integrated, energy-resolved neutron leakage spectrum for the Hiroshima device (Appendix D, Segment 41). The depicted leakage is normalized by a calculated device yield and further "bin-normalized" (divided by the energy bin width) so that it can be compared to the DS86 spectrum that used a different energy grid. Thus the units of the ordinate are *moles* kt^{-1} MeV^{-1}; the abscissa is in *MeV*.

The comparison shows that 200 energy bins provides more resolution than the 26 energy bins used in DS86. In particular, the effects of the elastic scattering resonance in iron are apparent (0.01 to 1 MeV), and there is now coverage below 20 eV.

Similarly, Figure 2 shows the energy-integrated, angle-resolved neutron leakage for the Hiroshima device (Appendix D, Segments 1 to 40). The depicted leakage is also normalized to a calculated yield and bin-normalized to permit comparison with DS86, which used a different angular grid. The units of the ordinate are *moles* kt^{-1} *unit-solid-angle*$^{-1}$; the units of the abscissa are $\cos(\theta)$, $-\pi \le \theta \le 0$. (A unit-solid-angle is simply a steradian divided by 2π and is equivalent to unit-cosine-in the polar direction.) The abscissa ranges from –1 (tail of the device) to 1 (nose of the device).

Again, the comparison shows strong similarities to DS86 with, perhaps, a slight shift in leakage from the nose toward the tail of the device.

Hiroshima Gamma Source

Figure 3 compares the angle-integrated, energy-dependent spectrum of the prompt gamma rays that leaked out of the Hiroshima device (Appendix E, Segment 41). The depicted leakage is normalized by a calculated device yield and further bin-normalized so that it can be compared to the DS86 spectrum, which used a different energy grid. Thus the units of the ordinate are *moles* kt^{-1} MeV^{-1}; the abscissa is in *MeV*.

There is a correspondence in the location of many leakage spectrum features. In particular, the average neutron energy is within 2% of the DS86 calculations (Table 1). However there is a 31% increase over DS86 in the total number of moles of prompt gamma rays. This may appear to be a significant change in the source terms until one realizes that the majority of the gamma-ray *dose* is produced from secondary and delayed gamma rays. These gamma rays are produced from neutron capture reactions and emission from the radioactive debris. Prompt gamma rays account for about 4% of the total gamma rays, and so it is seen that the increase in these calculations provides a roughly 1% increase in the total number of gamma rays. Whether it is an important change or not, it was a surprising change from DS86. The origin of the difference has been studied and is assessed to come from a recent physics improvement in the transport modeling. A "thick target bremsstrahlung" approximation for the photon production source is now included by default. Bremsstrahlung photons are produced in copious quantities, but because of their relatively lower energies, a fraction escape from the device.

Figure 4 shows the energy-integrated, angle-resolved gamma-ray leakage for the Hiroshima device (Appendix E, Segments 1 to 40). The depicted leakage is also normalized to a calculated yield and bin-normalized to permit comparison with DS86, which used a different angular grid. The units of the ordinate are *moles* kt^{-1} *unit-solid-angle*$^{-1}$; the units of the abscissa are cosines. The abscissa ranges from –1 (tail of the device) to 1 (nose of the device).

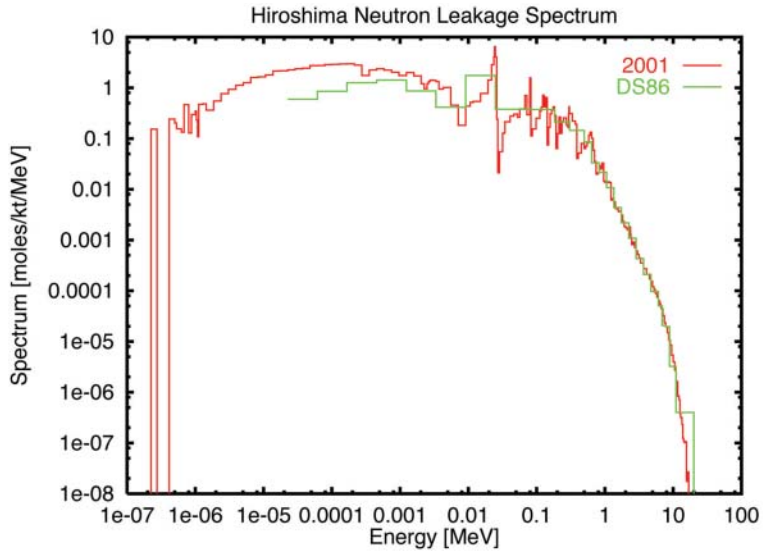

Figure 1. *Hiroshima angle-integrated neutron spectrum. The red curve is the 2001 calculation for DS02; the green curve is taken from DS86.*

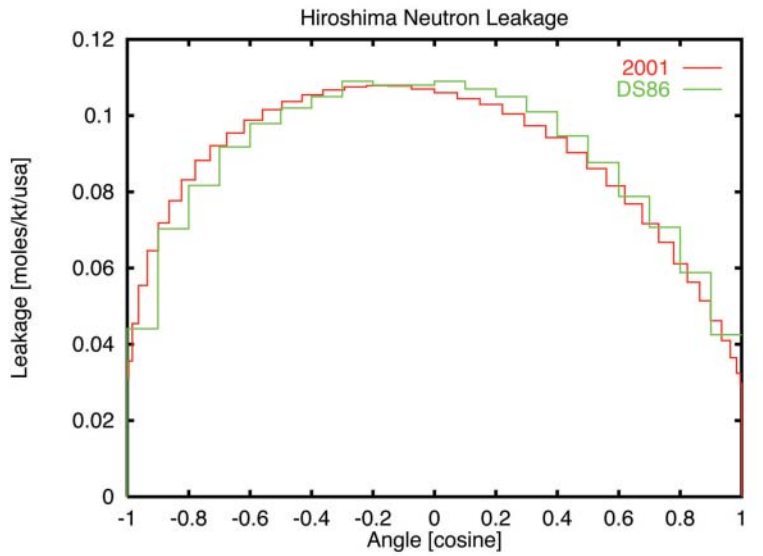

Figure 2. *Hiroshima energy-integrated neutron leakage. The red curve is the 2001 calculation for DS02; the green curve is taken from DS86.*

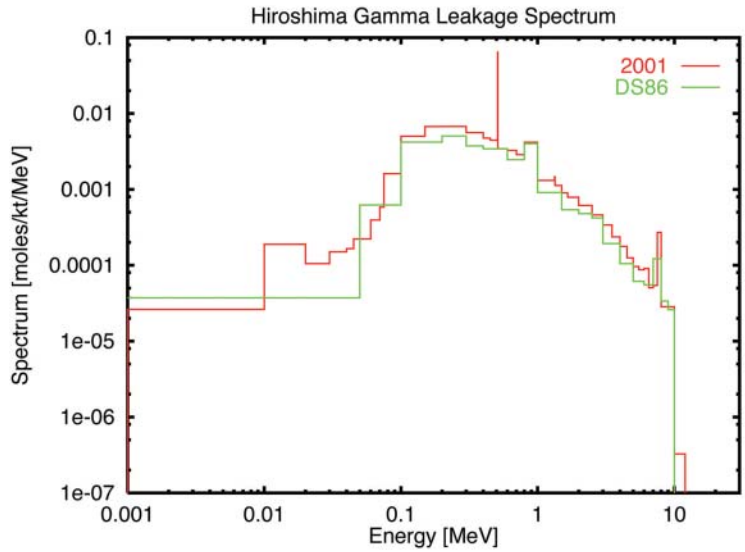

Figure 3. *Hiroshima angle-integrated gamma-ray spectrum. The red curve is the 2001 calculation; the green curve is taken from DS86.*

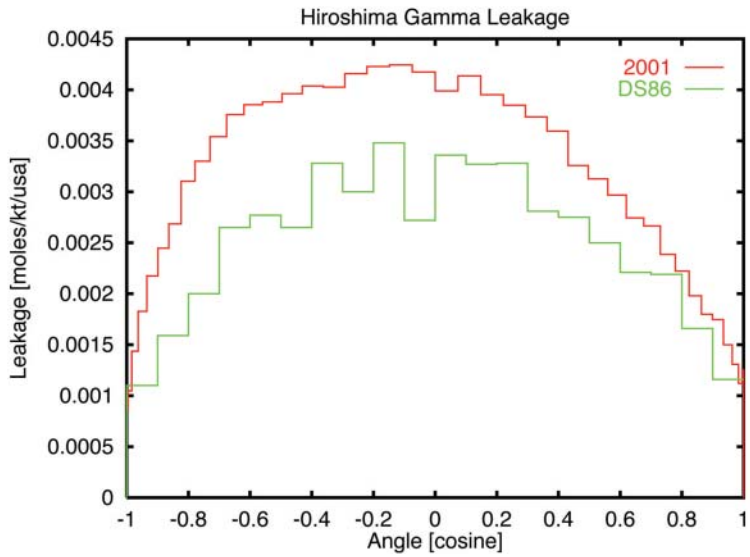

Figure 4. *Hiroshima energy-integrated gamma-ray leakage. The red curve is the 2001 calculation for DS02; the green curve is taken from DS86.*

The shapes of the gamma ray leakage curves are similar, and the increased magnitude in the current calculations is also apparent. In addition to bremstralung photons, the increased gamma-ray production can be attributed in part to (1) the longer time interval of one full second used in the DS02 calculations, (2) more complete modeling of the metal bomb casing in the geometry for the DS02 calculations, (3) the inclusion of higher energy gamma rays (between 10 and 20 MeV) not considered in DS86 calculations, and (4) changes in cross sections between the DS86 to the DS02 calculations.

Tilt Correction Equation

At the time of detonation, the Hiroshima bomb was not oriented vertically but was at an angle of 15 degrees to the vertical. The calculated neutron output from the bomb was not uniform in angle but had a distribution in which the output in the direction of the nose was quite suppressed. The transport of the radiation from the epicenter to the ground described below (LANSCE Calculations) is calculated in cylindrically symmetric coordinates, and does not take this tilt effect into consideration. The effect is limited in range. There is little asymmetry beyond 1,000-m slant range, and there is little effect anywhere for thermal neutrons. For a variety of reasons, principally the comparison to activation measurements, it is useful to have a correction for this effect. This correction is expressed as the ratio of the activation from a tilted calculation at a ground location to the activation at that location from an untilted calculation.

Table 2 describes tilt corrections from fits made by three-dimensional Monte Carlo calculations that asymptote to unity as the ground and slant ranges exceed 1,000 m. These fits come from new calculations that include the neutron kerma. The tilt corrections apply to the activation, A, not $S^2 \times$ A, where S is slant range. The corrections are in terms of X, the distance in meters from the hypocenter measured in the direction of the flight path. Figure 5 plots the fits.

Let Y be the direction normal to X, H be the height of burst, the ground range be $G = \sqrt{X^2+Y^2}$ and $S = \sqrt{G^2+H^2}$ be the slant range. Fits were tried in all of the variables X, Y, XY, X^2, Y^2 and S. Only the fits in S and X had statistical significance. The footprint of the neutron emission on the ground with no intervening scattering can be written in terms of S and X, the angle to the vertical of 15 degrees, and the angle of emission from the bomb $\mu = \cos(\varphi)$. The relation is $S\mu = H \cos(15) + X \sin(15)$. This provides a relation for contours on the ground at fixed values of μ as $Y^2 = \left((H \cos(15) + X \sin(15))/\mu\right)^2 - X^2 - H^2$. Figure 6 plots the iso-contours of the tilt correction for five values of μ.

Table 2. Tilt ratio table

	Equation parameter			Ratio Max-min	Relaxation length (m)	Number of mean-free-paths from a HOB of 600 m	$G_{6.5}$ (m)
	A	B	C				
^{32}S	85	1500	600	36.6%	162	3.7	865
^{63}Cu	45	1770	600	30.0%	153	3.9	793
Kerma	9.6	4200	550	11.3%	114	5.3	435
Thermal Ratio = 1				5.5%	93	6.5	0

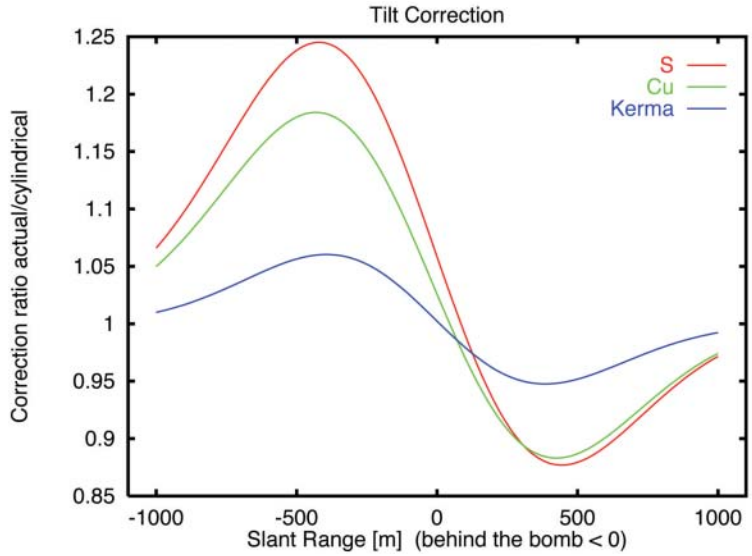

Figure 5. *Plot of the tilt correction for the tabulated reactions. In decreasing order of effect are* ^{32}S, ^{63}Cu *and kerma. The effect for thermal reactions is statistically insignificant and is not plotted.*

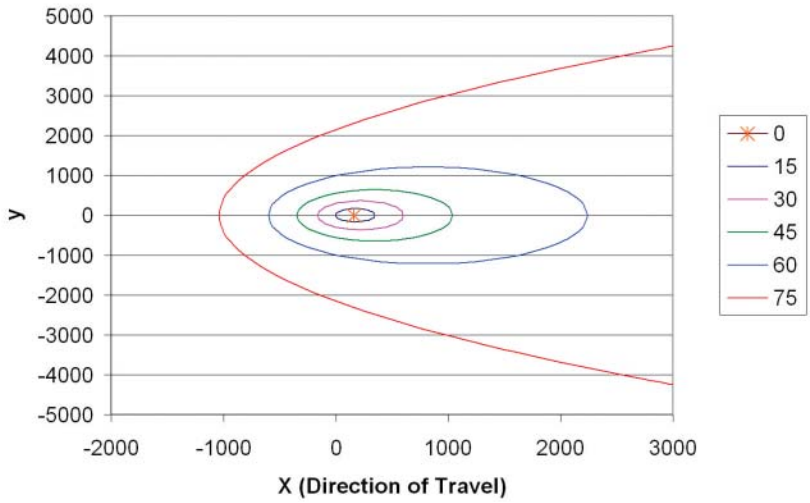

Figure 6. *Footprint of the neutron angular emission at HOB = 600 m with contours at 15, 30, 45, 60, and 75 degrees from the nose.*

The calculated tilt ratios for the thermal neutron reactions are all very small near the hypocenter, suggesting that scattering has smoothed out the neutron distribution. With this in mind we provide a table of tilt corrections that includes the coefficients of the correction and some other relevant quantities. The tilted-to-untilted correction is given by:

$$ratio(X) = 1 + (e^{-(X-A)/B} - 1)e^{-(X/C)^2}.$$

The columns labeled A, B and C are reaction-specific parameters in the ratio equation. The "max-min" quantity is *ratio* (–400 m) – *ratio* (400 m). The "relaxation length" is taken from the individual calculations. The average number of mean-free-paths is HOB/relaxation length. The ground range at a slant range of 6.5 mean-free-paths is shown in the $G_{6.5}$ column. The thermal value, 5.5%, is in the noise at 6.5 mean-free-paths calculated using the tabulated relaxation lengths.

LANSCE Calculations

As part of the effort to validate the Hiroshima-Nagasaki calculations, measurements of neutron transmission through the thick case material of a Hiroshima type bomb were made at the Weapon Neutron Research/Los Alamos Neutron Scattering Center (WNR/LANSCE) facility, formerly the Los Alamos Meson Physics Facility (LAMPF) (Nelson 2001). An intense white neutron source and long time-of-flight paths are available at the facility. Items of Hiroshima type hardened steel case material and internal mild steel components manufactured in the 1940's were available for the measurements.

Facility. At the WNR, a 2 μA current of 800-MeV protons produces neutrons upon striking a tungsten spallation target. The typical proton beam consists of 5×10^8 protons in 300 ps FWHM micro-pulses separated by 3.6 μs grouped in 650 μs macro-pulses, which are separated by 8.3 ms. In this experiment, neutrons were produced with energies between 0.65 MeV and 600 MeV. The typical neutron flux at the 20-m sample location was between 10,000 (at 1 MeV) and 3,000 (at 20 MeV) neutrons s^{-1} cm^{-2}. The neutron beam was collimated to 2.5-inch (6.35-cm) diameter.

Experiment. The transmission time-of-flight measurements were made with the 9-inch (22.9-cm) thick samples of hardened and mild steel at 20 m in the neutron flight path of 37.868 m to the plastic scintillator detector (E_n = 300 keV threshold). The sample faces were large compared to the neutron beam diameter. The neutron fluence was measured with a ^{238}U fission chamber in front of the samples at 19.34 m. The transmission was determined from the sample-in to sample-out ratio. Backgrounds were measured with 18-inch (45.7-cm) thick polyethylene absorbers at the sample position. Continuous energy Monte Carlo calculations are convolved with the detector system time response for comparison with measurements.

Results. An overview of the calculation-measurement comparison for the hardened case steel is shown in Figure 7 with more detailed comparisons in Figures 8 through 10. Neutrons are transmitted through hundreds of windows in the iron (Fe) of the steel case material and appear as peaks on the plots. The transmission is generally between 0.0005 and 0.01. The calculations with ENDF/B-VI.2 cross sections give results that are quite consistent with the WNR/LANSCE

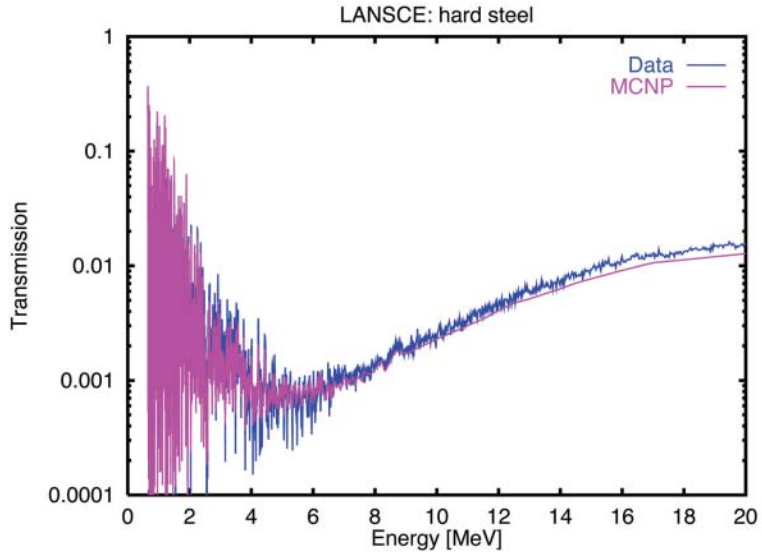

Figure 7. *Measured and calculated transmission for hard case steel and neutrons with energies from 0.65 to 20.65 MeV.*

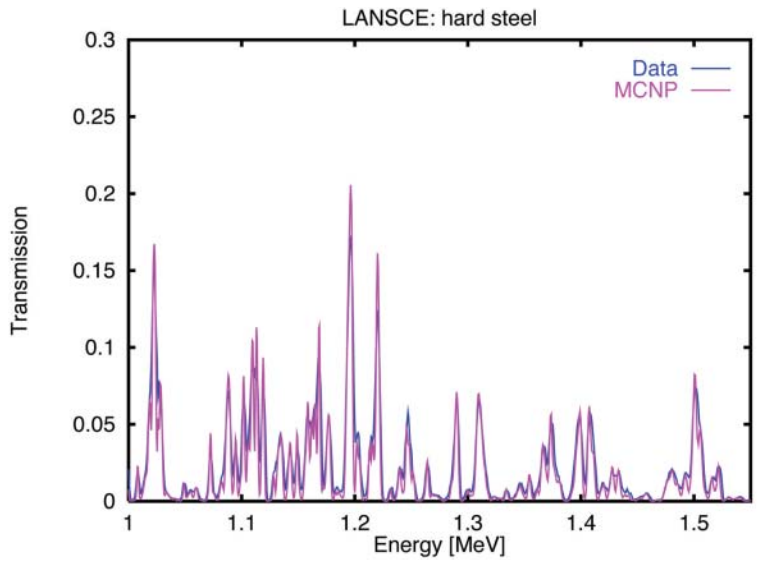

Figure 8. *Measured and calculated transmission for hard case steel, detail for neutrons with energies from 1.00 to 1.55 MeV.*

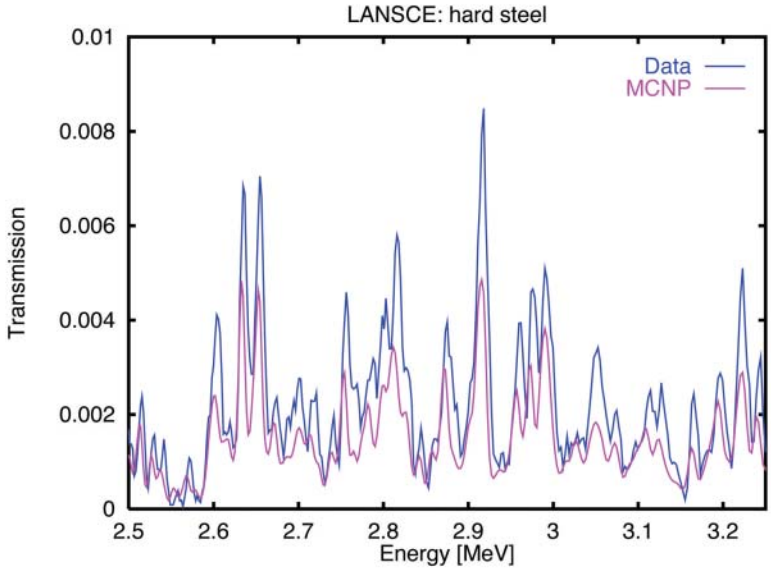

Figure 9. *Measured and calculated transmission for hard case steel, detail for neutrons with energies from 2.50 to 3.25 MeV.*

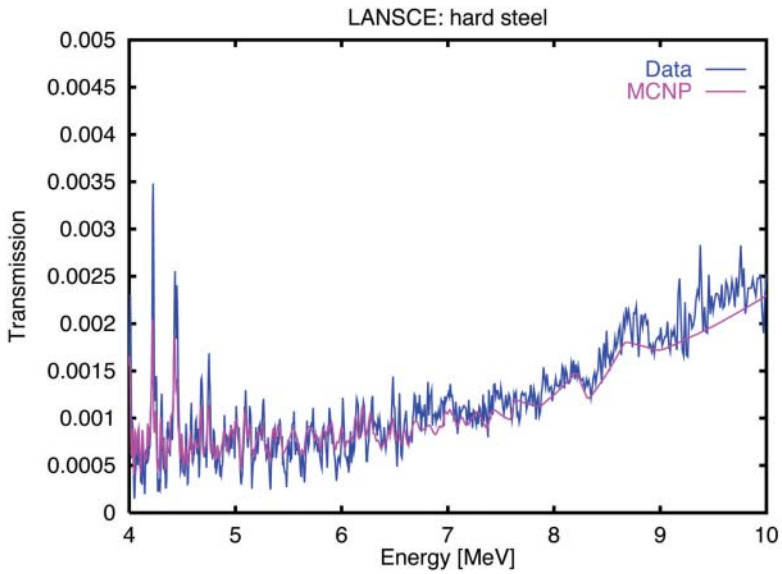

Figure 10. *Measured and calculated transmission for hard case steel, detail for neutrons with energies from 4.0 to 10 MeV.*

measurements as far as the location and shapes of the Fe windows in neutron energy space. The calculated magnitude of the transmission is in good agreement with the measurements from 0.65 to 2.0 MeV. From 2.0 to 20.0 MeV, the calculations fall below the measurements by an increasing percentage of approximately 35% at 10 MeV. The results from the mild steel comparison look almost the same as that shown for the hardened steel.

Implications. The transmission data described above were individually integrated over the energy bins used in the neutron source developed for the Hiroshima device. The energy range covered went from 0.65 MeV, the lower limit of the experiment, to 19.64 MeV, the upper limit of the source calculation's energy range. The ratio of the transmission measurement to the corresponding calculation over this range is 1.18; the ratio over the range from 1 to 4 MeV is 1.27. So it is apparent that the spectrum was perturbed. Activation calculations about the hypocenter were then re-run using a perturbed source scaled, bin-by-bin, with these transmission ratios.

The results of activation calculations for $^{63}Cu(n,p)^{63}Ni$, $^{32}S(n,p)^{32}P$, $^{59}Co(n,\gamma)^{60}Co$, $^{152}Eu(n,\gamma)^{153}Eu$ and $^{35}Cl(n,\gamma)^{36}Cl$ are shown in Figures 11 through 15. In all figures, activation as a function of slant range from the perturbed source calculation is co-plotted with that from the original source calculation.

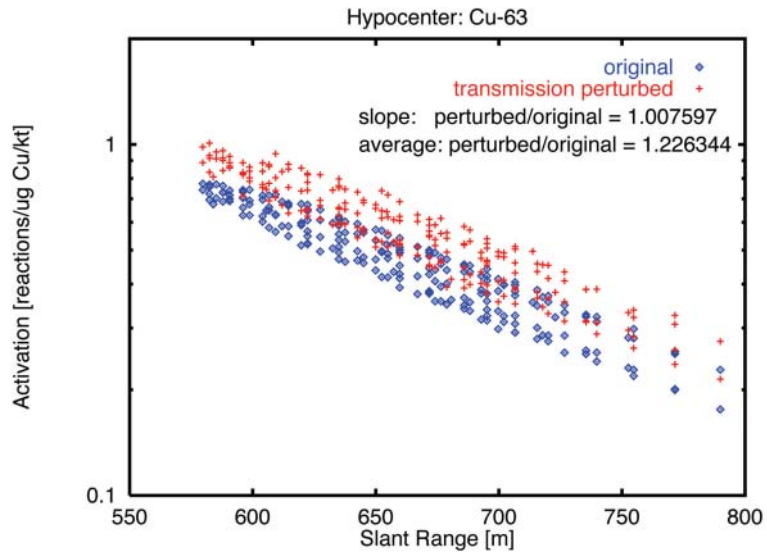

Figure 11. *Activation of ^{63}Cu from original and perturbed source vs slant range. Note that the "scatter" (multiple values at the same slant range) in this plot is caused by the 3-dimensional nature of the calculation which incorporates the "tilt" (bomb orientation) relative to the vertical. Locations below the nose of the bomb produce lower activations at the same slant range than locations off to the sides of the bomb. This effect is stongly apparent in activation reactions that reply on high energy neutrons.*

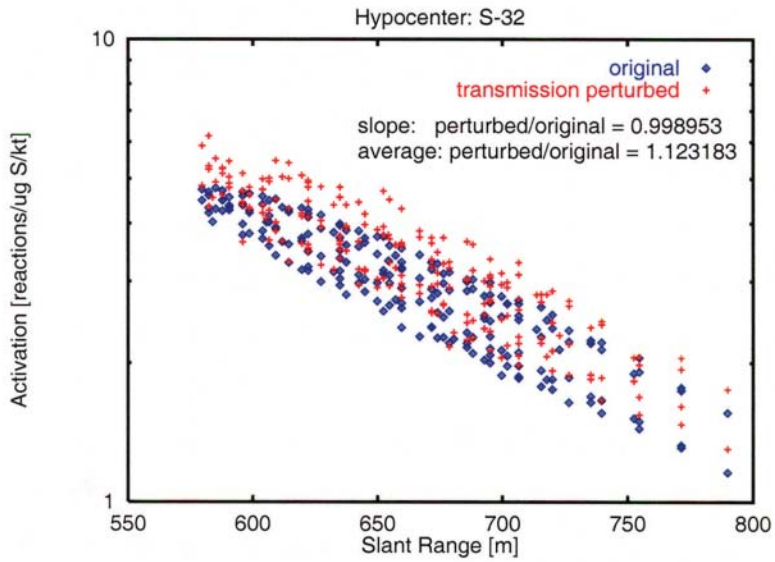

Figure 12. *Activation of ^{32}S from original and perturbed source vs slant range.*

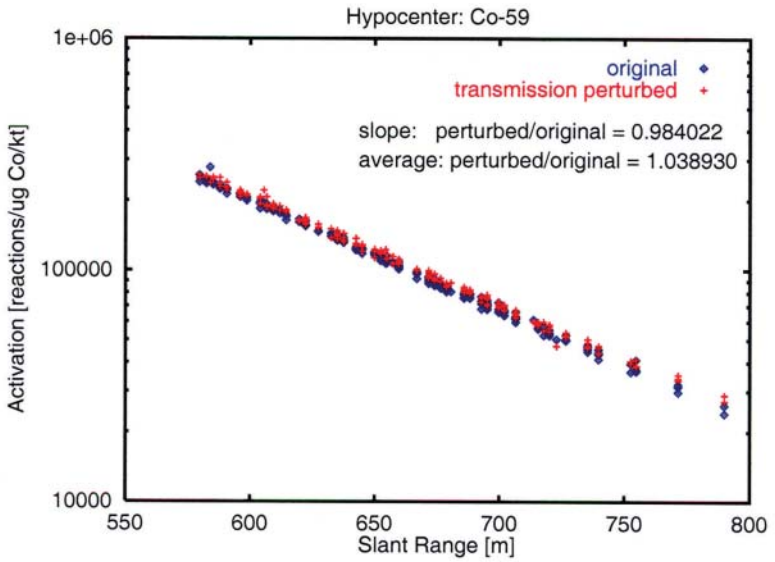

Figure 13. *Activation of ^{59}Co from original and perturbed source vs slant range.*

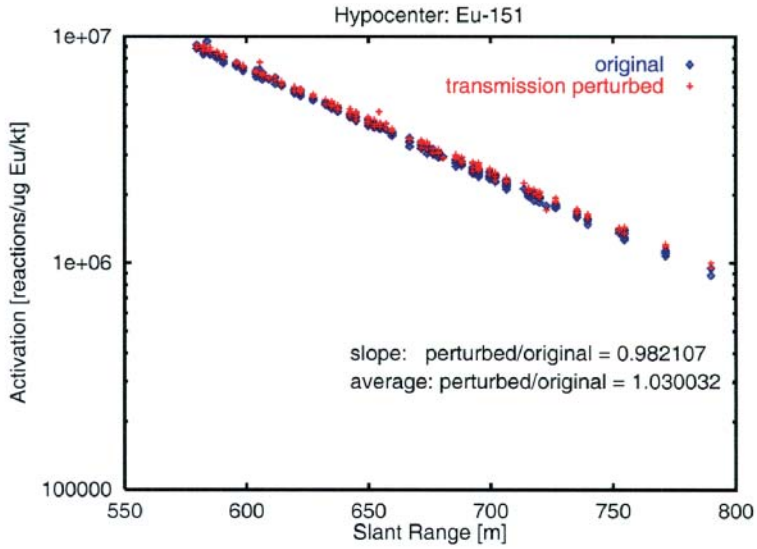

Figure 14. *Activation of ^{151}Eu from original and perturbed source vs slant range.*

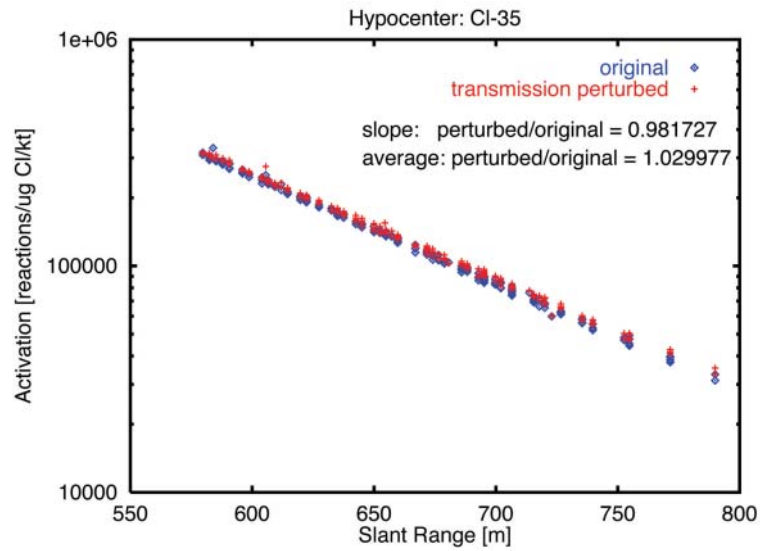

Figure 15. *Activation of ^{35}Cl from original and perturbed source vs slant range.*

The slope of a line fitted through the calculated points for each source description was calculated for six different activation products. The bottom line is that, while the magnitude of the activations sensitive to fast neutrons increased in about the proportion as the transmission ratio, it did not change for magnitude of the activations sensitive to thermal neutrons. Further the slope of the fitted lines did not change in any significant manner in either case. This suggests that an attempt to modify the source spectrum using data that could "resolve" cross-section uncertainties in the bomb case material does not change the slope of the line fitted through the activations in a manner that compares better with the trend in the measurements.

Hiroshima Bomb Calibration Calculations

To define the Hiroshima device neutron source, the neutrons born in the uranium fissile material must be calculated and transported through the moving material of the exploding bomb. There have been many cross-section changes between 1981 and 2001. A large number of cross section choices are now available for the major elements included in the device. To establish a baseline, a number of new calibration calculations were done, using the ENDF/B-VI.2 cross sections. These included criticality calculations of six static uranium critical assemblies and explosion calculations of three Nevada test devices.

The critical assemblies included the Little Boy Replica (Whalen 1984, 1987). The Little Boy Replica was assembled in 1982-1983 from non-fissile parts of a Hiroshima-type device stored from 1945 and newly fabricated fissile parts. Two sets of fissile parts were built for two distinct types of experiments. One set of fissile parts (1982) allowed the Little Boy Replica to be operated as a delayed critical reactor. Many measurements of the leakage neutron spectra were made using this delayed critical assembly (Whalen 1987). Another set of parts (1983) which duplicated the supercritical fissile parts of the Hiroshima bomb was used to make a modern critical separation measurement. The predicted yield from the critical separation experiment was 16 kt.

The Nevada test devices also included the Upshot-Knothole Grable shot (Glasstone 1962). The ENDF/B-VI.2 cross sections resulted in a closer grouping of calculations to measurements than previously achieved in studies of these various weapon tests and static uranium critical assemblies.

Nagasaki Neutron Source

The Nagasaki device geometry is significantly different from that of the Hiroshima device. The principal effect of this difference is that the neutron and gamma-ray leakages from this goemetry are isotropic to within the accuracy of calculations. It is, therefore, unnecessary to provide detailed angular resolution for the leakage quantities.

Figure 16 shows the energy-resolved neutron leakage spectrum for the Nagasaki device (Appendix F). The depicted leakage is normalized by a calculated device yield and further bin-normalized so that it can be compared to the DS86 spectrum that used a different energy grid. Thus the units of the ordinate are *moles* kt^{-1} MeV^{-1}; the abscissa is in *MeV*.

An initial impression of this comparison suggests significant differences between the new sources and DS86. Table 1, however, indicates that, in an integral sense, there is only about a 3% decrease in the number of prompt neutrons leaked. In fact at energies above 10^{-2} MeV, the new data track DS86 with differences generally attributable to the more resolved energy bin structure.

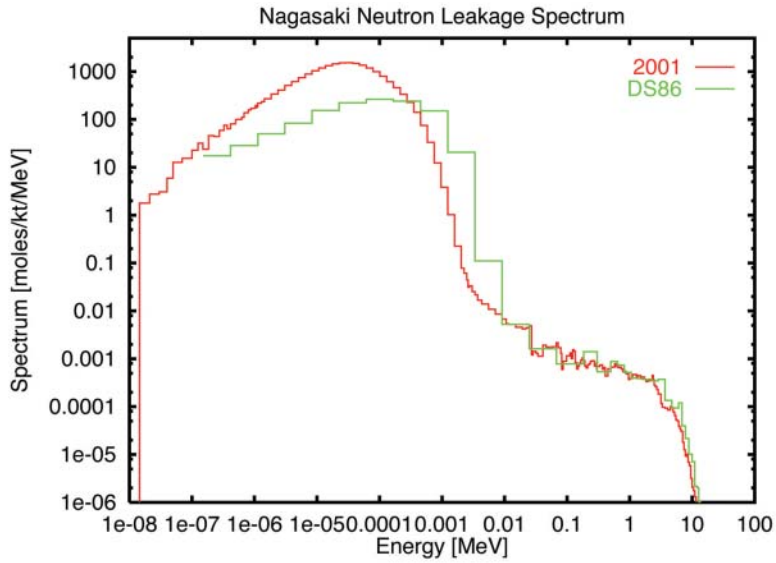

Figure 16. *Nagasaki neutron spectrum. The red curve is the 2001 calculation for DS02; the green curve is taken from DS86.*

Below 10^{-2} MeV there is a distinct shift in the thermal peak toward lower energies in the new spectrum. It is asserted that this difference occurs because the greater temporal extent in the new calculations has allowed the high explosive material to elastically downscatter neutrons to these lower energies. The significance of this is that, even at these energies, there will be little additional neutron flux on the ground because very few will travel far from the epicenter with that energy. The mean-free-path in air for 2 to 4 MeV neutrons is roughly an order of magnitude larger than that for neutrons below 10^{-2} MeV.

Nagasaki Gamma Source

Figure 17 shows energy-dependent spectrum of the prompt gamma rays that leaked out of the Nagasaki device (Appendix G). The depicted leakage is normalized by a calculated device yield and further bin-normalized so that it can be compared to the DS86 spectrum that used a different energy grid. Thus the units of the ordinate are *moles* kt^{-1} MeV^{-1}; the abscissa is in *MeV*.

There is a correspondence in the location of many leakage features. In particular the average energy is within 6% of the DS86 calculations. However, there is a 43% increase over DS86 in the total number of moles of prompt gamma rays. This result is very similar to that observed in the Hiroshima prompt gamma-ray calculations, but there are subtle differences at higher gamma-ray energies that contribute importantly to survivor doses. For example, there are 8.4 times more gamma rays at energies above 5 MeV in the DS02 Nagasaki output than there were in the DS86 calculation, whereas there is only a 28% increase at gamma-ray energies above 5 MeV in the DS02 Hiroshima output compared to DS86. The reasons for this large increase in higher energy

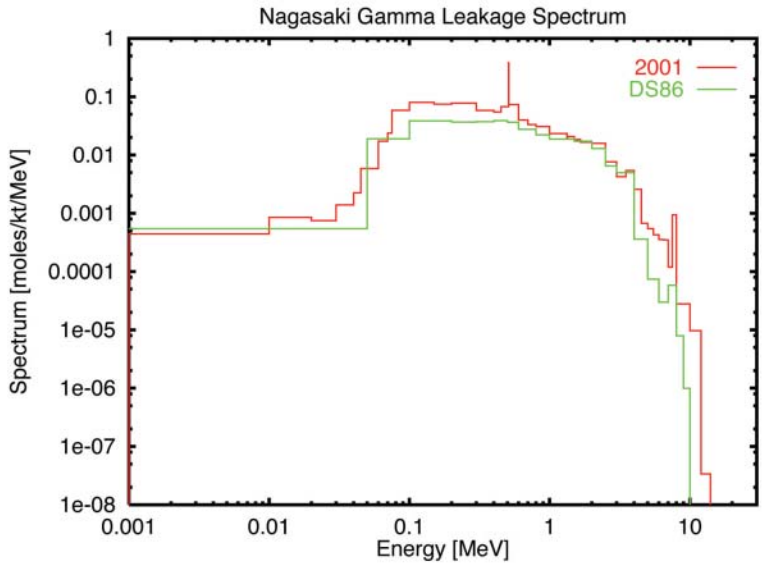

Figure 17. *Nagasaki gamma ray leakage. The red curve is the 2001 calculation for DS02; the green curve is taken from DS86.*

gamma rays at Nagasaki have not been fully investigated, but it is probably attributable to (1) recent changes in nitrogen cross sections, (2) the inclusion of more metal parts of the bomb case in the geometry for the DS02 calculation, (3) the running of the DS02 calculation to longer times (approximately 1 second) allowing for more nitrogen capture to occur in the high explosives of the Nagasaki bomb, and (4) the inclusion of 10-20 MeV gamma rays in the DS02 calculation (including the 11-MeV gamma rays from nitrogen capture).

Conclusions

A new set of calculations for the neutron and gamma outputs of the Hiroshima and Nagasaki atomic bombs has been provided. Generally, where there is overlap, there is good agreement between these calculations and those reported in DS86. The new calculations, however, contain more extensive reporting resolution and improved geometry.

Acknowledgements

The authors would like to thank Charles H. Aldrich, III, Los Alamos National Laboratory, for the design calculation of the Nagasaki bomb.

References

Bond, V. P.; Thiessen, J. W.; eds. *Reevalulations of Dosimetric Factors: Hiroshima and Nagasaki.* Oak Ridge, Tennessee: Washington, D.C.: U.S. Department of Energy; DOE Symposium Series 55; CONF-810928 (DE81026279); 1982.

Glasstone, S.; ed. *The Effects of Nuclear Weapons.* Washington, D.C.: U.S. Department of Defense and U.S. Atomic Energy Commission; 1962.

Hendricks, J. S.; Frankle, S. C.; Court, J. D. *ENDF/B-VI Data for MCNP*. Los Alamos, New Mexico: Los Alamos National Laboratory; LA-12891; December 1994.

McVane, V.; Dunford, C. L.; Rose, P. F.; eds. *ENDF-102: Data Formats and Procedures for the Evaluated Nuclear Data File ENDF-6*. Upton, New York; Brookhaven National Laboratory; BNL-NCS-44945 Revised; 1995.

Nelson, R. O.; Bliss, J.; Morgan, G.; Abfelterer, W.; Ragan, C. E. Unpublished presentation: Little Boy Transmission Measurements at WNR/LANSCE, May 10-11, 2001.

Preeg, W. E. "Neutron and Gamma-Ray Output for Fat Man and Little Boy: Letter to C.P. Knowles dated April 5, 1976." In: *Reevaluations of Dosimetric Factors: Hiroshima and Nagasaki*; pp. 125-130 (Bond, V. P.; Thiessen, J. W.; eds.). Washington, D.C.; U.S. Department of Energy; DOE Symposium Series 55; CONF-810928 (DE81026279); 1982.

Whalen, P. P. "Source Terms for the Initial Radiations." In: *First US-Japan Joint Workshop on Reassessment of Atomic Bomb Radiation Dosimetry in Hiroshima and Nagasaki*, pp. 13-14 (Thompson, D. J.; ed.). Hiroshima, Japan: Radiation Effects Resarch Foundation; 1983.

Whalen, P. P.; Soran, P. D.; Malenfant, R.; Forehand, H. M., Jr. "Experiments at Los Alamos National Laboratory with the Replica of the Hiroshima Bomb." In: *Second US-Japan Joint Workshop on Reassessment of Atomic Bomb Radiation Dosimetry in Hiroshima and Nagasaki*, pp. 21-25 (Kato, H.; et al.; eds). Hiroshima, Japan: Radiation Effects Resarch Foundation; 1983.

Whalen, P. P. "Calculation and Verification of Source Terms." In: *US-Japan Joint Reassessment of Atomic Bomb Radiation Dosimetry in Hiroshima and Nagasaki, Final Report, Vol. 1*, pp. 37-65 (Roesch, W. C.; ed.). Hiroshima, Japan: Radiation Effects Research Foundation; 1987.

Whalen, P. P. "Source and Replica Calculations." In: *Eighth Internaional Conference on Radiation Shielding, Vol. 1*, pp. 212-223. La Grange Park, Illinois: American Nuclear Society; 1994.

White, J. E.; Ingersoll, D. T.; Wright, R. Q.; Hunter, H. T.; Slater, C. O.; Greene, N. M.; MacFarland, R. E.; Roussin, R. W. *Production and Testing of the Revised VITAMIN-B Fine-Group and the BUGLE-96 Broad-Group Neutron/Photon Cross-Section Libraries Derived from ENDF/B-VI.3 Nuclear Data.* Oak Ridge, Tennessee: Oak Ridge National Laboratory; ORNL/TM-6795/R1; April 2000.

White, S. W. Los Alamos National Laboratory, Private communication (e-mail) with Dean Kaul, Science Applications International Corporation, February 2002.